ARTICLES

Electrons weakly bound to hydrogen bonded clusters: A pseudopotential model including dispersion interactions

Milan Šindelka, Vladimír Špirko, and Pavel Jungwirth[a)]
J. Heyrovský Institute of Physical Chemistry, Academy of Sciences of the Czech Republic and Center for Complex Molecular Systems and Biomolecules, Dolejškova 3, 18223 Prague 8, Czech Republic

(Received 18 April 2002; accepted 18 June 2002)

A pseudopotential model for the description of binding of an excess electron to polar clusters or molecules is presented. In addition to Coulomb, short range repulsion, and polarization interactions between the excess electron and the neutral core, the model also accounts for dispersion within a second order perturbation treatment. The pseudopotential, which should enable future dynamical calculations coupling the excess electron with nuclear motions, is successfully tested against accurate *ab initio* results for a whole set of geometries of hydrogen fluoride dimer anion. Predictions are made for an electron bound to a collinear hydrogen fluoride trimer for different values of the intermonomer separations. For the optimal and shorter values of this separation two bound states of the excess electron in $(HF)_3^-$ are predicted to exist. © *2002 American Institute of Physics.* [DOI: 10.1063/1.1499486]

I. INTRODUCTION

Excess electron, i.e., an additional electron weakly bound to molecular or cluster systems with a filled valence shell, is an interesting quantum object with many unusual properties, reminiscent of a delocalized character of Rydberg electrons to a certain extent. The binding of the excess electron is, however, due to its Coulomb interactions with *higher* multipoles (dipole, quadrupole, etc.) of the closed shell neutral ''core'' and/or polarization and dispersion forces. The extended body of theoretical and experimental studies concerning molecular and cluster dipole bound anions has been summarized in two recent reviews.[1,2] As typical examples of cluster systems, hydrogen fluoride dimer and water dimer have been predicted to possess a sufficiently large dipole moment to bind an excess electron already in the 1970s.[3,4] In both cases, this has later been verified experimentally, and it has been established that the weak binding of the excess electron to such hydrogen bonded dimers is of the order of 50 meV.[5–7]

Historically, two theoretical approaches for the description of dipole bound anions have been developed. The first approach treats the excess electron as a dynamical quantum particle separated from the electrons of the neutral core, with which it interacts via a more or less empirically parameterized pseudopotential.[8–11] These pseudopotentials typically contain three terms, describing the electrostatic (charge-dipole and possibly also charge-quadrupole) interactions, short range electron-neutral core repulsion, and polarization of the neutral system by the excess electron.

Several of the pseudopotential models for an excess electron attached to a molecule or a cluster[9,11] assume the neutral system to be a symmetric top with a dipole moment placed along the principal symmetry axis. The problem then acquires a cylindrical symmetry with only two electronic degrees of freedom, the distance r from the center of the neutral core and angle θ between the direction of r and that of the dipole moment. A rotationally adiabatic potential $V_{ad}(r)$ for the excess electron is calculated as the lowest eigenvalue of the Hamiltonian

$$\hat{H}=\hat{H}_{\mathrm{rot}}+\hat{l}^2/2r^2+V(r,\theta). \tag{1}$$

Here, $\hat{H}_{\mathrm{rot}}$ is the rotational Hamiltonian of the neutral system, $\hat{l}$ is the relative angular momentum operator of the electron with respect to the molecule or cluster, and $V(r,\theta)$ is the electron-neutral system pseudopotential. Within the rotationally adiabatic approximation the excess electron binding energy is obtained by solving the radial Schrödinger equation with the lowest rotationally adiabatic potential.[9,11]

The second strategy for treating dipole bound anions is based on an *ab initio* quantum chemistry approach.[2] This methodology on the one hand incorporates the excess electron into the electronic structure of the whole system, while on the other hand invokes the Born–Oppenheimer separation between electronic and nuclear motions. The Born–Oppenheimer approximation is well justified if the excess electron motion is much faster than that of the rotating and vibrating nuclei. Except for excess electron states with less than roughly 1 meV binding energy or highly excited nuclear rotational or vibrational states, this condition is usually well fulfilled.[12,13] The advantage of treating the electronic structure of the whole dipole bound anion is that, in principle, a numerically exact Born–Oppenheimer solution of the electronic problem can be obtained. In practice, extended basis sets with a large amount of diffuse functions as well as ad-

a)Electronic mail: jungwirt@jh-inst.cas.cz

vanced electronic structure methods [such as coupled cluster with singles, doubles and perturbative triples—CCSD(T)] are required to obtain reliable values for the excess electron binding.[2,14–21] As a consequence, accurate calculations are currently numerically feasible only for small or moderately sized systems.

Recently, a Drude model approach to the binding of excess electrons in dipole bound anions was developed.[22,23] The excess electron interacts with the neutral core via a model potential, partially parameterized via *ab initio* calculations. Polarization and dispersion interactions are accounted for via Drude oscillators representing the neutral systems. Note that dispersion, which can contribute up to 50% of the excess electron binding [e.g., to $(H_2O)_2$ or $(HF)_2$ clusters] was not included into previous pseudopotential models. The Drude approach employs quantum chemistry methods (perturbation expansion or configuration interaction) for a reduced dimensionality system Drude oscillator(s)-excess electron, which makes it practical for rather large molecules or clusters. The recent results for anionic water clusters are very encouraging in this respect.[23]

In our recent study, we investigated dipole bound anions from the point of view of possible couplings between the motions of the excess electron and nuclear motions of the neutral core.[13] Namely, for the case of hydrogen fluoride dimer anion we focused on the hydrogen bond donor–acceptor interchange tunneling which reverses the dipole moment of $(HF)_2$. Since the excess electron binds at the positive end of the dimer dipole, it moves from one side of the dimer to the other during the nuclear tunneling motion. We have shown that for a vibrationally and rotationally cold cluster such a ''double tunneling'' can be described within the Born–Oppenheimer approximation.[13] However, upon vibrational excitation the separation between nuclear motions and that of the excess electron is no longer valid. In the long run, we aim for a fully coupled description of the dynamics of the excess electron and selected relevant nuclear vibrational and tunneling degrees of freedom. This goal is clearly beyond the Born–Oppenheimer approximation and, therefore, excludes the direct use of traditional *ab initio* techniques.

In the present paper we outline a pseudopotential model for the excess electron which would enable nonadiabatic dynamical studies. It is tailored in particular to electrons dipolarly bound to hydrogen bonded clusters, however, it can be quite generally used for excess electrons in molecules, clusters, and possibly also condensed phases. The present model is based on older pseudopotentials,[8–11] however, it also accounts for dispersion interactions. Dispersion is included without invoking Drude oscillators, in the spirit of the pseudopotential treatment of core-valence dispersion in heavy atom systems.[24,25] For cluster systems, the pseudopotential is constructed from monomer contributions, similarly to a recent study of the water dimer anion.[12] The accuracy of the present pseudopotential is tested against high level *ab initio* calculations for the intermolecular potential energy surface of hydrogen fluoride dimer anion and for the optimal geometry of the $(HF)_3^-$ cluster. The rest of the paper is organized as follows. In Sec. II we outline in detail the pseudopotential model and in Sec. III we describe the methodology for calculating bound and continuum wave functions of the excess electron. Section IV contains computational details. Results of our calculations are presented and discussed in Sec. V, while Sec. VI contains concluding remarks. A detailed analysis of orthonormality relations of continuum wave functions of the excess electron is given in the Appendix.

II. PSEUDOPOTENTIAL MODEL

The present pseudopotential is tailored primarily to the description of an excess electron in polar clusters. For an arbitrary cluster, possessing generally no symmetry, we start with expanding the electron-cluster pseudopotential into electron-monomer contributions:

$$V(\mathbf{r}) = \sum_{j=1}^{N} V_j(\mathbf{r}), \tag{2}$$

where $\mathbf{r}$ is a position vector of the excess electron in a space fixed coordinate frame with the origin at the center of mass of the neutral system, and N is the number of monomers (molecules or atoms) forming the cluster.

Each of the contributions V_j has the functional form:

$$V_j(\mathbf{r}) = V_j^{sr}(\mathbf{r}) + V_j^{lr}(\mathbf{r}). \tag{3}$$

The long range part of the electron-monomer pseudopotential V_j^{lr} has an electrostatic part V_j^{es} and a polarization term V_j^{pol}. For a general nonsymmetric monomer the electrostatic interaction can be represented as a sum of electron-partial charges terms, with fractional charges (typically placed on the monomer atoms) representing the neutral monomer charge density. For a symmetric top monomer one can alternatively use a simple multipolar expansion (truncated at the quadrupolar term):

$$V_j^{es}(\mathbf{r}) = \left(-\frac{\mu_j \cos(\theta_j)}{r_j^2} - \frac{Q_j(3\cos^2(\theta_i)-1)}{2r_j^3} \right) f_d(r_j). \tag{4}$$

The electron coordinates r_j and θ_j are defined with respect to the center of mass principal axis orientation of the monomer and can be easily expressed in terms of the original electron coordinates $\mathbf{r}$ and monomer nuclear coordinates, both with respect to a space fixed coordinate frame. f_d is a short range damping function (the exact form of which is given below), μ_j is the monomer dipole and Q_j quadrupole moment. We have realized that in order to increase the accuracy of the pseudopotential we should allow the monomers to polarize each other, especially for small intermonomer separations. Empirically, we have found that this small correction can be satisfactorily accounted for by a simple formula

$$\mu_j = \mu_j^0 \left(1 + \sum_{j \neq i} A_{ij} e^{-B_{ij} R_{ij}} \cos \gamma_{ij} \right), \tag{5}$$

where μ_j^0 is the dipole moment of an isolated monomer, γ_{ij} is the angle between dipole moments of monomers i and j, R_{ij} is the intermonomer separation, and A_{ij} and B_{ij} are fitting constants.

For a symmetric top monomer the polarization term V_j^{pol} can be expressed as follows (for an asymmetric monomer the expression is also straightforward, albeit slightly more complicated):

$$V_j^{\mathrm{pol}}(\mathbf{r}) = \left(-\frac{\alpha_j^{\parallel}\cos^2(\theta_j)}{2r_j^4} - \frac{\alpha_j^{\perp}(1-\cos^2(\theta_j))}{2r_j^4} \right) f_d(r_j), \tag{6}$$

where $\alpha_j^{\parallel}$ is the component of monomer polarizability parallel and $\alpha_j^{\perp}$ perpendicular to the principal molecular axis of the monomer.

For principal reasons there is no entirely satisfactory way how to define the short range repulsion term, $V_j^{sr}(\mathbf{r})$. This term results from electron–electron interactions at small separations and a pseudopotential which separates the excess electron from valence electrons simply cannot do full justice to the electron exchange. Several empirical terms have been employed in the past. An exponential short range term can be written as:[12]

$$V_j^{sr}(\mathbf{r}) = \exp(-(r_j/r_c)^6), \tag{7}$$

where r_c is an adjustable parameter. Alternatively, a polynomial form can be postulated:[11]

$$V_j^{sr}(\mathbf{r}) = (-\alpha_j^{\parallel} r_j^{\parallel 4}\cos^2(\theta_j)/2r_j^8 - \alpha_j^{\perp} r_j^{\perp 4}(1-\cos^2(\theta_j))/2r_j^8), \tag{8}$$

where $r_j^{\parallel 4} = C\alpha_j^{\parallel 1/3}$, $r_j^{\perp 4} = C\alpha_j^{\perp 1/3}$, and C is and adjustable parameter close to unity.[11] In the present pseudopotential we employ the above polynomial form of the short range term.

Eigenvalues and eigenvectors of the excess electron Hamiltonian $\hat{H}_e$

$$\hat{H}_e = \hat{T}_e + \sum_{j=1}^{N} (V_j^{sr}(\mathbf{r}) + V_j^{lr}(\mathbf{r})) \tag{9}$$

are calculated using a close coupling scheme which is described in detail in the next section and in the Appendix. An important point is, that not only the lowest eigenfunction of the excess electron, but also excited functions, mostly corresponding to continuum states, are evaluated. This allows then to account for the dispersion contribution to the excess electron binding. The dispersion energy is calculated in a similar way as the core-valence dispersion contribution in heavy atom pseudopotential models.[24,25]

The dispersion contribution from monomer j within a second order perturbation treatment is given as:[24]

$$V_j^{\mathrm{disp}} = -\frac{1}{2}\alpha_j \int_0^{\infty} dE |\langle \psi_0(\mathbf{r}) | \mathcal{E}_j(\mathbf{r}) | \psi_E(\mathbf{r}) \rangle|^2 \times \frac{\Delta E_j}{\Delta E_j + (E - E_0)}. \tag{10}$$

Here, α_j is the mean polarizability of the given monomer, and $\mathcal{E}_j(\mathbf{r}) = e(\mathbf{r}-\mathbf{r}_j)/|\mathbf{r}-\mathbf{r}_j|^3$ is the electric field created by the excess electron at the mass center $\mathbf{r}_j$ of the monomer. ΔE_j is the mean excitation (Unsöld) energy of the monomer, usually taken as its first ionization potential. As a matter of fact, the results are robustly insensitive to the particular choice of ΔE_j, since the energy ratio in Eq. (10) is always very close to unity for significantly contributing energies of the excess electron. E_0 is the ground state energy, $\psi_0(\mathbf{r})$ represents the ground state wave function, and the integration runs over all energies E of continuum states $\psi_E(\mathbf{r})$ of the excess electron, as described in detail in the next subsection.

In principle, one should also add discrete contributions from excited bound states of the excess electron. We discuss this issue in detail later; here it suffices to say that systems with a moderate dipole moment (such as water dimer or hydrogen fluoride dimer anions) possess only one well developed bound state. Some larger clusters with huge dipole moments can have more than one bound state of the excess electron. In that case the contribution from these states to dispersion should be included, too, similarly as in Eq. (10), replacing, however, integration with a discrete sum. Finally, the total dispersion energy is given as a sum of all excess electron-monomer contributions:

$$V^{\mathrm{disp}} = \sum_{j=1}^{N} V_j^{\mathrm{disp}}. \tag{11}$$

In this paper, we apply the pseudopotential model to an excess electron bound to small hydrogen fluoride clusters. For this system the following numerical values of parameters of the HF monomer entering into the pseudopotential have been adopted: $\mu^0 = 0.7174$, $Q = 1.7719$, $\alpha^{\parallel} = 6.380$, $\alpha^{\perp} = 4.962$, $A = 7.068$, $B = 0.781$, and $C = 1.195$. All of the above parameters are in atomic units. The first four parameters of the neutral HF monomer have been obtained directly from *ab initio* calculations (at the MP2/aug-cc-pvtz level), while the last three constants have been taken as fitting parameters. The damping function takes the form $f_d(r) = 1 - \exp[-(r/r_0)^6]$, where we have fixed $r_0 = 1$ a.u. not including it into the set of fitting parameters. Finally, we recall that the equilibrium HF bond length is $R = 1.755$ a.u.

III. EXCESS ELECTRON WAVE FUNCTIONS

A. Bound and continuum state wave functions

When calculating the wave functions of the excess electron we are dealing with bound and continuum states of the three dimensional Schrödinger equation

$$\left[-\frac{\hbar^2}{2m_e}\Delta + V(\mathbf{r}) \right] \psi(\mathbf{r}) = E\psi(\mathbf{r}), \tag{12}$$

where $V(\mathbf{r})$ is the pseudopotential of the excess electron. Bound state solutions of Eq. (12) correspond to the discrete part of the eigenvalue spectrum. Discrete index ν is used to label different bound state eigensolutions $\psi_\nu(\mathbf{r})$ and the corresponding eigenenergies E_ν. Bound state wave functions satisfy the standard orthonormality relations

$$\langle \psi_\nu | \psi_{\nu'} \rangle = \int_{\mathbf{R}^3} \psi_\nu^*(\mathbf{r})\psi_{\nu'}(\mathbf{r})d\mathbf{r} = \delta_{\nu\nu'}, \tag{13}$$

where $\delta_{\nu\nu'}$ denotes the Kronecker delta function.

Each energy level from the continuum part of the spectrum is infinitely degenerate. Discrete index ξ is used to label different linearly independent eigensolutions with given energy E, therefore, in actual calculations summation over in-

dex ξ has to be added in Eq. (10). Continuum wave functions, $\psi_{E\xi}(\mathbf{r})$, are assumed to satisfy the generalized orthonormality relations

$$\langle \psi_{E\xi} | \psi_{E'\xi'} \rangle = \int_{\mathbf{R}^3} \psi^*_{E\xi}(\mathbf{r}) \psi_{E'\xi'}(\mathbf{r}) d\mathbf{r} = \delta(E-E') \delta_{\xi\xi'} \tag{14}$$

with $\delta(E-E')$ denoting the Dirac delta function. A detailed analysis of the above orthonormality relations is presented in the Appendix.

B. Close coupling expansion

A conventional spherical harmonic expansion of the excess electron wave function is employed,

$$\psi(\mathbf{r}) = \frac{1}{r} \sum_q R_q(r) Y_q(\hat{r}). \tag{15}$$

Here $\hat{r}$ denotes the angular coordinates ϑ and φ and symbol q stands for a collective index labeling the pair of quantum numbers (l_q, m_q) of the spherical harmonics function Y_q. Using the expansion (15), the eigenproblem (12) is transformed into a system of coupled differential equations for the radial components $R_q(r)$. It holds

$$-\frac{\hbar^2}{2m_e}\frac{d^2}{dr^2}R_q(r) + \frac{\hbar^2 l_q(l_q+1)}{2m_e r^2} R_q(r) + \sum_{q'} V_{qq'}(r) R_{q'}(r) = E R_q(r), \tag{16}$$

where

$$V_{qq'}(r) = \int Y^*_q(\hat{r}) V(\mathbf{r}) Y_{q'}(\hat{r}) d\hat{r}. \tag{17}$$

In matrix notation, Eq. (16) may be equivalently rewritten as follows:

$$\left[-\frac{\hbar^2}{2m_e}\frac{d^2}{dr^2} \otimes \mathbf{I} + \mathbf{L}(r) + \mathbf{V}(r) \right] \mathbf{R}(r) = E\mathbf{R}(r). \tag{18}$$

We note explicitly that $[\mathbf{L}(r)]_{qq'} = \delta_{qq'} \hbar^2 l_q(l_q+1)/2m_e r^2$, the meaning of other matrix symbols being evident from Eq. (16).

The dispersion contributions $\langle \psi^{(1)}(\mathbf{r}) | \mathcal{E}_j(\mathbf{r}) | \psi^{(2)}(\mathbf{r}) \rangle$ [see Eq. (10)] are expressed in terms of radial components $R_q(r)$ as

$$\langle \psi^{(1)}(\mathbf{r}) | \mathcal{E}_j(\mathbf{r}) | \psi^{(2)}(\mathbf{r}) \rangle = \sum_q \sum_{q'} \int_0^\infty [R^{(1)}_q(r)]^* \mathcal{E}^{qq'}_j(r) R^{(2)}_{q'}(r) dr. \tag{19}$$

Here $\psi^{(1)}(\mathbf{r})$ and $\psi^{(2)}(\mathbf{r})$ represent the bound and continuum state eigenfunctions and

$$\mathcal{E}^{qq'}_j(r) = \int Y^*_q(\hat{r}) \mathcal{E}_j(\mathbf{r}) Y_{q'}(\hat{r}) d\hat{r}. \tag{20}$$

C. Boundary conditions

It is important to choose proper boundary conditions for the radial wave functions. The inner boundary condition requires that all the components of the column vector $\mathbf{R}(r=0)$ should be zero. The outer boundary condition, imposed on the asymptotic behavior of $\mathbf{R}(r\to\infty)$, takes for the bound states a completely different functional form than for the continuum states. In the bound state energy region $E<0$, radial components $R_q(r\to\infty)$ should decay exponentially as $\exp[-\kappa r]$ with $\kappa = (1/\hbar)\sqrt{-2m_e E}$. In the continuum energy region $E>0$, radial components $R_q(r\to\infty)$ oscillate asymptotically as $\sin(kr+d_q)$ with $k = (1/\hbar)\sqrt{2m_e E}$.

Due to the fact that each continuum energy level is infinitely degenerate, various equivalent outer boundary conditions may be introduced, making different conventions for definition of single linearly independent eigensolutions. Most frequently, two particular choices of the boundary conditions appear in the literature. Both of them employ spherical Bessel functions $\mathsf{j}_l(x)$, $\mathsf{n}_l(x)$, $\mathsf{h}^{(\pm)}_l(x)$ (for explicit definitions see, e.g., Ref. 26). The first convention assumes that the ξth linearly independent continuum eigenfunction takes the asymptotic form

$$[R^{E\xi}_q(r)/r](r\to\infty) \approx \sqrt{\frac{2m_e k}{\pi\hbar^2}} \{ \mathsf{j}_{l_q}(kr)\delta_{q\xi} + \mathsf{n}_{l_q}(kr) K^{E\xi}_q \}. \tag{21}$$

Here quantities $K^{E\xi}_q$ represent the elements of the real and symmetric $\mathbf{K}$-matrix of the scattering theory. According to the second convention

$$[R^{E\xi}_q(r)/r](r\to\infty) \approx \sqrt{\frac{m_e k}{2\pi\hbar^2}} \{ \mathsf{h}^{(-)}_{l_q}(kr)\delta_{q\xi} - \mathsf{h}^{(+)}_{l_q}(kr) S^{E\xi}_q \}, \tag{22}$$

where quantities $S^{E\xi}_q$ represent the elements of the complex and unitary $\mathbf{S}$-matrix of the scattering theory. It is worth noting that the asymptotic form (22) implicitly assures the validity of generalized orthonormality relations (14). In the case of the boundary conditions (21), relations (14) are not satisfied and an additional orthonormalization procedure must be introduced. Detailed discussion of this point can be found in the Appendix. In the present study, we have adopted the convention (21), which allows us to work with real functions.

IV. COMPUTATIONAL DETAILS

All cluster geometries considered in the present study exhibit some degree of symmetry; in particular, the clusters belong to $C_{\infty v}$, $D_{\infty h}$, or C_s point groups. Standard techniques of group theory enable construction of symmetry adapted angular bases as linear combinations of spherical harmonics. System (18) of differential equations is then separated into uncoupled subsystems, each of them being associated with a certain column of a given irreducible representation of the corresponding point group. Introduction of this procedure enables us to considerably cut down the dimensionality of the corresponding coupled channel problems and, therefore, to enormously reduce the CPU time required for running the calculations. When evaluating the dispersion contributions according to Eqs. (10) and (19), it is important to take into account the fact that the operators $\mathcal{E}_j(\mathbf{r})$ exhibit different symmetry properties than the cluster itself. Consequently, the matrix elements $\langle \psi^{(1)}(\mathbf{r}) | \mathcal{E}_j(\mathbf{r}) | \psi^{(2)}(\mathbf{r}) \rangle$ are in

TABLE I. The cutoff $l_{\max}$ together with the number N_{term} of coupled equations for different symmetry groups employed.

Point group	$l_{\max}$	N_{term}
$C_{\infty v}$	30	30
$D_{\infty h}$	50	25
C_s	9	55

general nonzero even if the wave functions $\psi^{(1)}(\mathbf{r})$ and $\psi^{(2)}(\mathbf{r})$ belong to different irreducible representations.

The close coupling expansion (15) was truncated at some finite value of $l=l_{\max}$. The appropriate cutoff $l_{\max}$, which is sufficient for satisfactory numerical convergence of the results, depends significantly on symmetry and anisotropy of the cluster. In addition, the higher the symmetry of the cluster, the larger the value of $l_{\max}$ may be chosen, keeping the number of coupled equations within an acceptable range. Table I displays the employed values of $l_{\max}$ together with typical numbers of coupled equations N_{term}. The relatively low degree of symmetry (C_s) of the nonlinear dimer allows to perform only moderate factorization. Consequently, a lower value of $l_{\max}$ is employed here than for collinear geometries, where results are fully converged. Results obtained for $l_{\max}=9$ can be safely regarded as quantitative, although they are not fully converged. Error estimates are of the order of 3%–4% in this case.

The truncated system of coupled equations (18) for the bound/continuum eigenstates was solved numerically on a discrete radial grid using the renormalized Numerov method as described in Ref. 27. For calculations involving the physically relevant strongly bound states, the radial grid included $G=4000$ points extending equidistantly from $r_0=0$ up to $r_{\max}=200$ a.u. with the increment $h=0.05$ a.u. In order to illustrate contributions of marginally bound states, an extremely large grid, characterized by the parameters $r_{\max}=100\,000$ a.u., $G=400\,000$ points, and increment $h=0.25$ a.u., was necessary.

Two-dimensional integrals (17) and (20) have been calculated via the Gauss–Legendre quadrature scheme,[28] using typically about 50 mesh points for the spherical angle $\vartheta \in \langle 0,\pi)$ and about 100 mesh points for the spherical angle $\varphi \in \langle 0,2\pi)$. One-dimensional integration in Eq. (19) was performed simply by summation over all the radial grid points. The integration over the continuum energy region [see Eq. (10)] followed again the Gauss–Legendre scheme. The interval $E \in (0.0,10.0$ a.u.) was divided into several subintervals with different densities of the quadrature points. The total number of considered continuum energy levels did not exceed 500.

V. RESULTS AND DISCUSSION

Within the Born–Oppenheimer approximation the charge-dipole potential supports, for dipoles larger than a critical value of approximately 1.625 D, an infinite number of bound states of the excess electron.[29–31] However, binding energies of these states approach exponentially zero. As a result, almost all of these states disappear upon relaxing the Born–Oppenheimer separation between the excess electron and nuclear motions. Consequently, dipolarly bound anions typically have one or at most several bound states.[31] For example, small polar clusters such as water dimer or hydrogen fluoride dimer support just a single bound state of the excess electron.

Our long term computational goal is to enable nonadiabatic calculations, coupling the excess electron to nuclear vibrations. The idea is to couple first the nuclear and the electronic degrees of freedom using a pseudopotential without accounting for dispersion interactions, and include the dispersion term *ex post* within a second order perturbative treatment. In the present paper, however, we evaluate the dispersion term using adiabatic states of the excess electron. A methodological question arises whether to include into the dispersion calculation also contributions from excited bound states of the excess electron. It is an experimentally confirmed fact[7] that the hydrogen fluoride dimer supports only one bound excess electron state, all the others being artefacts of the Born–Oppenheimer approximation. Before answering the above question we have evaluated the ground and two lowest excited Born–Oppenheimer states of the excess electron in $(HF)_2$ for a collinear geometry with optimal F–F distance of 2.7 Å. The energies (without dispersion) of the three states are 30.1, 0.053, and 0.000 095 meV, decreasing, indeed, exponentially. The three radial wave functions (integrated over the angular coordinates) are depicted in Fig. 1. We see immediately that the excited wave functions are spatially extremely extended, much more than the already diffuse ground state wave function. This indicates that the coupling between the ground and excited bound states via the electric field operator may be very small. This indeed turns out to be the case and calculations show that the contribution of the excited bound states to the dispersion is vanishing (less than 0.01% for the first and 0.0001% for the second excited state). Thus, we conclude that in $(HF)_2^-$ only continuum states contribute to the dispersion term which makes the problem connected with the artificiality of the excited bound states irrelevant. Finally, contributions ΔE_{disp} of continuum states of particular energies to dispersion are shown in Fig. 2. The curve peaks close to zero energy, although the threshold continuum states with almost no energy do not contribute to dispersion. The dispersion contributions then decrease with increasing energy of continuum states, however, states with up to 50 eV contribute non-negligibly.

In the next step we have evaluated the binding energy of the excess electron for a whole set of geometries of hydrogen fluoride dimer. Namely, we have varied the F–F distance and the two H–F–F angles, fixing the monomer H–F distances at their equilibrium value and keeping the whole complex planar. A general planar geometry of $(HF)_2$ together with these geometric parameters is shown in Fig. 3. As benchmarks, we have employed the Hartree–Fock level for calculations without dispersion, and the CCSD(T) level of theory for calculations including the dispersion term. Exactly as in our previous study[13] we have augmented a standard aug-cc-pvdz basis set with five very diffuse *sp* sets approaching thus basis set convergence for the excess electron binding (at least for geometries around the optimal structure).

Figure 4 shows the excess electron binding for collinear

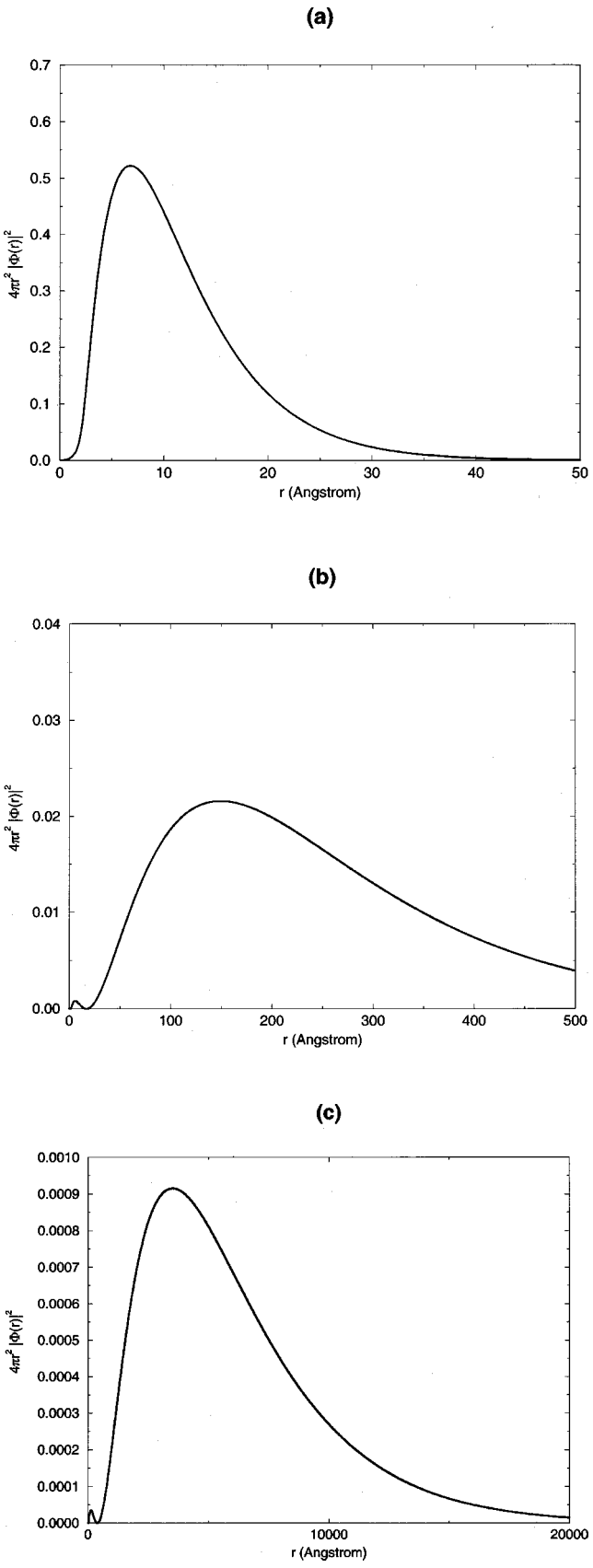

FIG. 1. The radial probabilities of the (a) ground, (b) first excited, and (c) second excited wave function of an excess electron bound to a collinear hydrogen fluoride dimer with optimal F–F separation of 2.7 Å. Note the different scales on the axes of the three figures and the fact that the actual grid employed in the calculations is much more extended than shown in the figure.

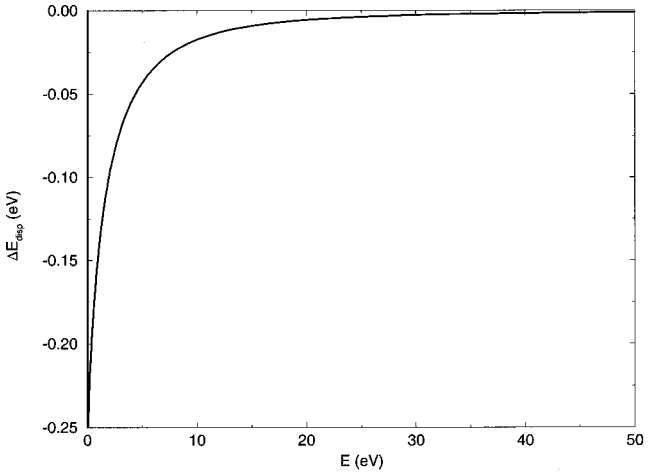

FIG. 2. Contributions ΔE_{disp} of continuum states with energies ranging from 0 to 50 eV to dispersion interaction between a collinear $(HF)_2$ cluster with F–F distance of 2.7 Å and an excess electron.

geometries of the cluster varying the F–F distance. We see that the present pseudopotential energy without dispersion matches almost exactly the Hartree–Fock energies. This agreement has been achieved by fitting only three parameters-A and B, characterizing mutual polarization of the two HF monomers, and the repulsive constant C [see Eqs. (5) and (8)]. From Fig. 4(b), which compares the present calculations with dispersion to CCSD(T) values, it can be seen that the present model performs satisfactorily, overestimating the excess electron binding energy by at most 10% for the whole range of studied F–F separations. We stress that this agreement has been obtained without any additional fitting. It might seem a bit surprising that the present model, which accounts for dispersion only within a second order perturbation treatment, compares so well to CCSD(T). The reason is, that for $(HF)_2^-$ all the higher terms above MP2$disp$ almost perfectly cancel, at least for geometries close to the minima of both anionic and neutral hydrogen fluoride dimers.[15] The abbreviation MP2$disp$ means including into the binding energy above the Hartree–Fock level only the second order dispersion term (see Ref. 15). It is possible, that in other systems the cancellation of the higher terms will be less good, which would then influence the accuracy of the present model.

Geometries corresponding to bending of the H–F–F angles (keeping the F–F distance at 2.7 Å) are depicted in Figs. 5 and 6. It is satisfying that a satisfactory performance of the present model extends also to bent geometries. The in-plane bending motions are the two crucial degrees of freedom involved in the donor–acceptor interchange tunneling,[13] and the current pseudopotential should be thus capable of

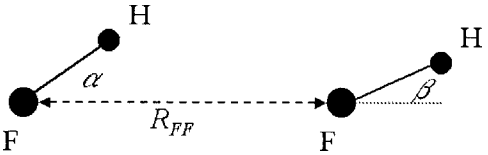

FIG. 3. General geometry of the hydrogen fluoride dimer with explicit definition of the three geometric parameters varied in the calculations.

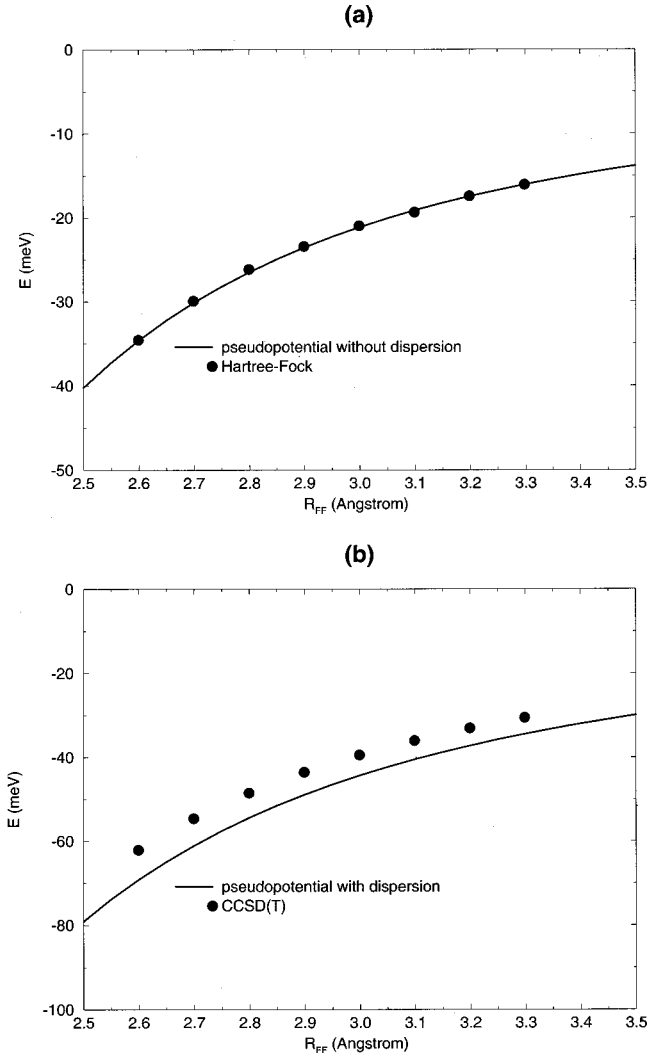

FIG. 4. Binding energy of the excess electron as a function of the F–F distance for a collinear hydrogen fluoride dimer. Comparison between (a) pseudopotential without dispersion and Hartree–Fock, and (b) pseudopotential with dispersion and CCSD(T).

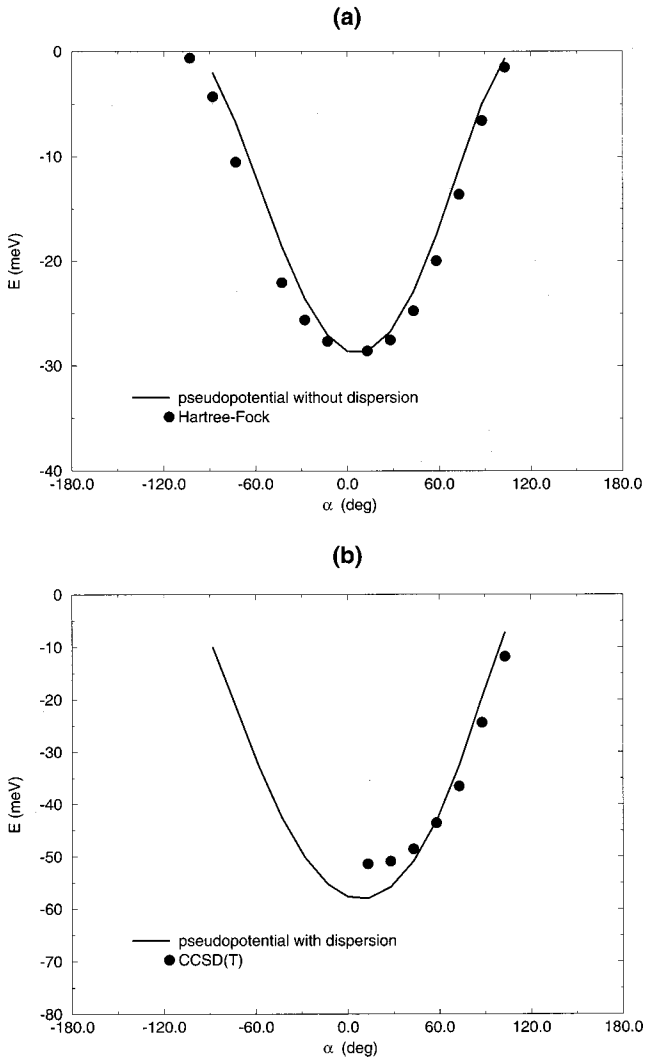

FIG. 5. Binding energy of the excess electron as a function of the H–F–F angle α for $R_{FF}=2.7$ Å and $\beta=3°$. Comparison between (a) pseudopotential without dispersion and Hartree–Fock, and (b) pseudopotential with dispersion and CCSD(T).

describing the accompanying concerted dynamics of the nuclei and the excess electron. In Figs. 5 and 6 we vary one of the H–F–F angles in the range between roughly −120 and 120 deg (positive values corresponding to *cis* and negative to *trans* geometries). The second angle has been fixed at a small value of 3 or 13 deg.

We do not show comparison between the pseudopotential and *ab initio* calculations for larger values of the second angle since for these geometries the latter exhibit severe convergence problems. This is due to the fact that for strongly bent geometries the dipole moment of the neutral core decreases and eventually the excess electron becomes unbound. While in this situation the pseudopotential binding energy smoothly approaches zero from below, the Hartree–Fock energy can become even positive [see points corresponding to large values of the first H–F–F angle in Fig. 6(a)] and CCSD(T) does not converge. Problems with convergence are also behind the fact that we present in Figs. 5(b) and 6(b) CCSD(T) results only for positive values of the H–F–F angle α.

The above artifact of the Hartree–Fock calculation is clearly due to the fact that a marginally bound excess electron is extremely delocalized and, consequently, the basis set becomes insufficient. Within the all electron *ab initio* approach it is then necessary to add extra diffuse functions, which not only makes the calculations significantly more time consuming (post-Hartree–Fock methods scale with the number of basis functions as polynomials of order six or higher) but can also cause severe convergence problems. Within the one electron pseudopotential treatment it is, however, relatively easy and straightforward to extend the radial range of the basis (or grid).

Figure 7 deals with F–H···H–F collinear geometries upon varying the F–F distance. These geometries are unstable due to the antiparallel orientation of the HF monomer dipoles, however, they are interesting from the point of view of a possible support of a ''solvated electron'' state between the two monomers[16] (clearly, the solvated electron states become more relevant for large clusters and for the liquid bulk). Although the present pseudopotential has been devel-

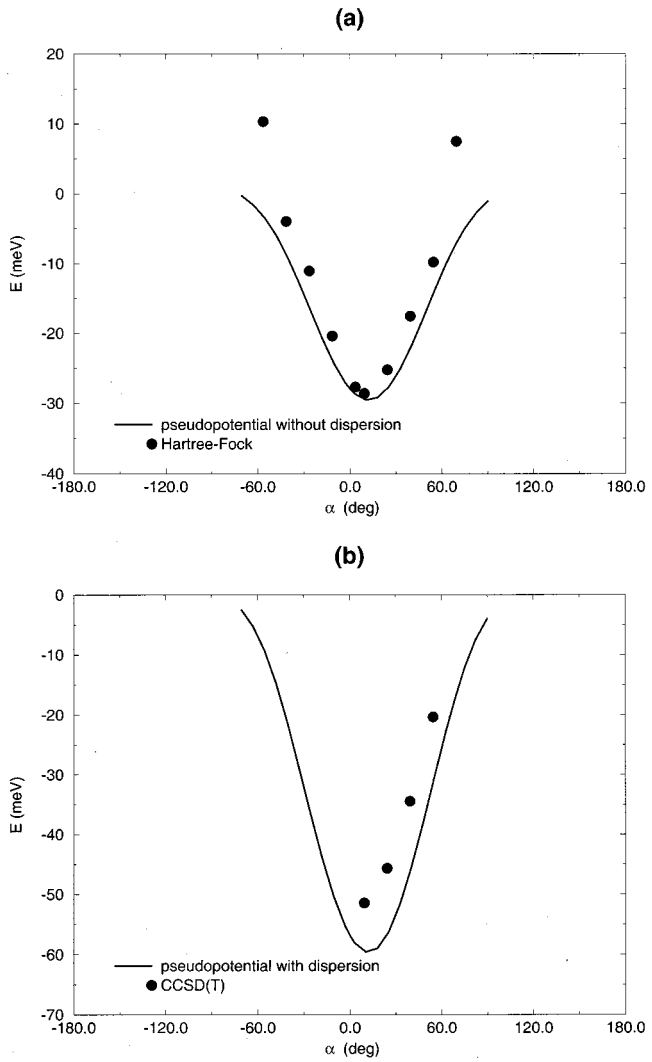

FIG. 6. Binding energy of the excess electron as a function of the H–F–F angle α for $R_{FF}=2.7$ Å and $\beta=13°$. Comparison between (a) pseudopotential without dispersion and Hartree–Fock, and (b) pseudopotential with dispersion and CCSD(T).

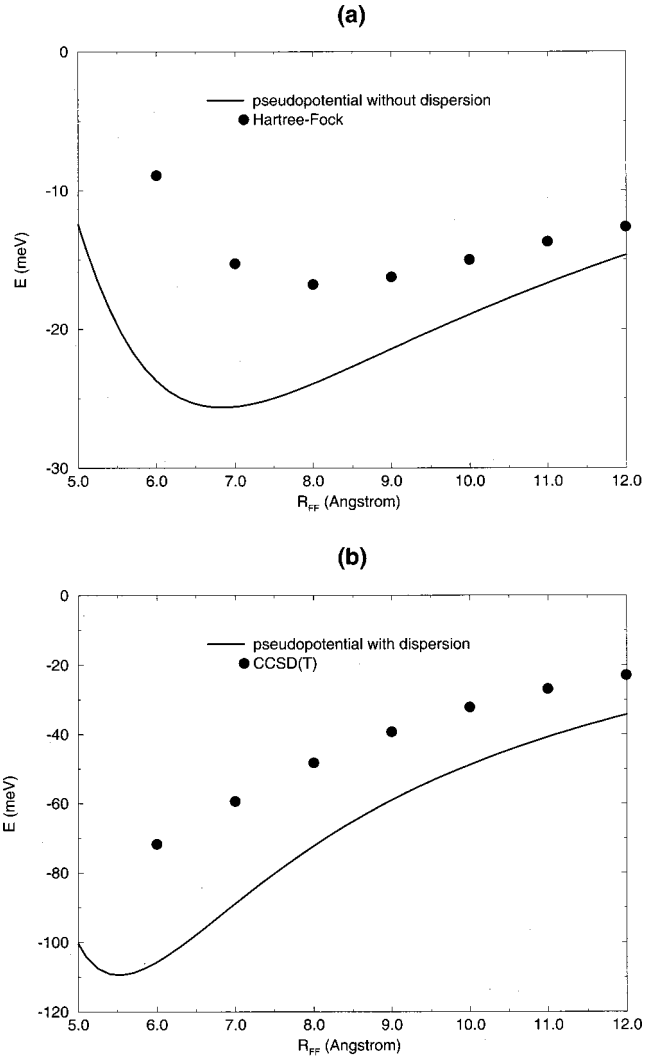

FIG. 7. Binding energy of the excess "solvated" electron as a function of the F–F distance for a collinear hydrogen fluoride dimer in the F–H···H–F arrangement. Comparison between (a) pseudopotential without dispersion and Hartree–Fock, and (b) pseudopotential with dispersion and CCSD(T).

oped for the dipole bound rather than solvated electron, we see that it qualitatively works also for the latter case. The overall change of the solvated electron binding upon F–F stretching is captured by the pseudopotential, which, however, overestimates the total electron binding by about 50% (or a factor of 2 without dispersion).

As a next step, we have applied the present pseudopotential without any adjustments to an electron dipolarly bound to hydrogen fluoride trimer. As an example, Fig. 8 shows the excess electron binding energy along the symmetric intermolecular stretch of a collinear cluster. On Fig. 8 the favorable comparison of pseudopotential results without dispersion to Hartree–Fock values (difference of the order of 10%) is demonstrated. We also see that, compared to the dimer, binding increases more than three times, which is primarily due to a significantly larger dipole moment of the HF trimer. As a matter of fact, for F–F separations equal or smaller than the optimal value of 2.7 Å the system supports also a well developed excited excess state. The energy profile of the excited excess electron along the symmetric F–F stretch is shown in Fig. 9. Of course, this excited state is much more weakly bound than the ground state. However, with binding energy of several meVs, this excited state is likely to exist even beyond the Born–Oppenheimer approxi-

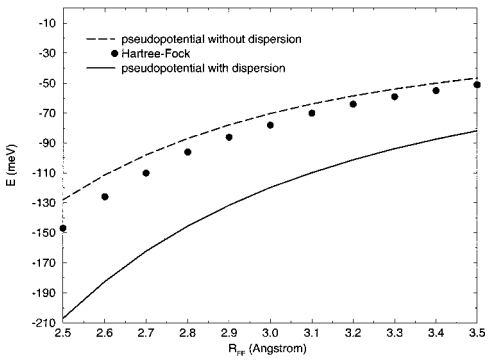

FIG. 8. Binding energy of the excess electron as a function of the F–F distance for a collinear hydrogen fluoride trimer. Results employing pseudopotential with and without dispersion are presented. The latter are compared to Hartree–Fock calculations.

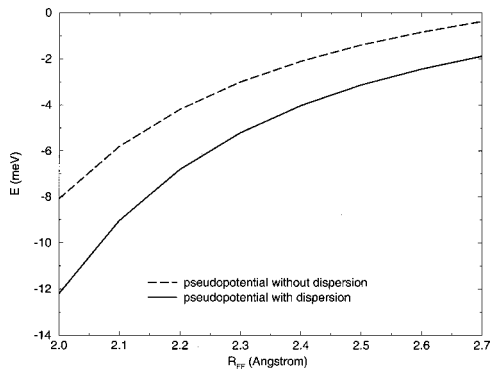

FIG. 9. Binding energy of the excess electron in the first excited state as a function of the F–F distance for a collinear hydrogen fluoride trimer. Results employing pseudopotential with and without dispersion are presented.

mation. Finally, we note that the energy of the ground state at F–F separations of 2.7 Å without (or with) dispersion also compares favorably (within 10%) to the *ab initio* HF (or MP2*disp*) energy of the optimized, slightly noncollinear HF trimer anion.[16]

VI. CONCLUSIONS

A pseudopotential model, which should enable future studies of a nonadiabatic dynamics coupling nuclear motions with that of the excess electron bound to polar clusters or molecules, has been developed. The model builds on earlier pseudopotentials adding, however, also a dispersion term. Dispersion is accounted for within a second order perturbation treatment similarly as in the case of core-valence pseudopotentials. The model, which involves only three fitting parameters, performs quantitatively for a whole set of geometries of hydrogen fluoride dimer anion. Without any additional fitting, good results are obtained also for an excess electron bound to hydrogen fluoride trimer. For optimal and shorter intermonomer separations of the collinear $(HF)_3^-$ cluster two bound states of the excess electron are predicted to exist.

ACKNOWLEDGMENTS

We are grateful to Shai Ronen, Professor Jiří Formánek, and Professor Felicia Mrugala for useful discussions. Support from the Volkswagen Stiftung (Grant No. I/75908) and from the Czech Ministry of Education (Grant No. LN00A032) is gratefully acknowledged.

APPENDIX: ORTHONORMALITY RELATIONS

The present section contains a detailed analysis of the orthonormality relations (14). We provide a thorough discussion of this point for two reasons. First, a rigorous treatment of orthonormality is crucial for correct evaluation of the dispersion contributions. Second, although appropriate formulation for the one-dimensional problems is well-known, its generalization to the coupled channel systems is not completely trivial, since each continuum energy level possesses a degeneracy which equals to the number of coupled equations. We were unable to find such an explicit generalization in available literature. The treatment described below is closely related to that outlined by Child[32] for the case of a one-dimensional eigenproblem.

Let us examine the properties of overlap integrals

$$I_L(E,\xi,E',\xi')=\int_{\Omega_L}\psi^*_{E\xi}(\mathbf{r})\psi_{E'\xi'}(\mathbf{r})d\mathbf{r}, \tag{A1}$$

with the integration range Ω_L being a sphere of radius L. These integrals are continuous functions of independent variables E, E' and L.

After a substitution of the spherical harmonics expansion (15), followed by an analytic integration over $\hat{r}$, Eq. (A1) is transformed as

$$\begin{aligned} I_L(E,\xi,E',\xi') &= \sum_q \int_0^L [R_q^{E\xi}(r)]^* R_q^{E'\xi'}(r)dr \\ &= \int_0^L [\mathbf{R}^{E\xi}(r)]^{*T}\mathbf{R}^{E'\xi'}(r)dr \\ &= \int_0^L [\mathbf{R}^{E'\xi'}(r)]^T[\mathbf{R}^{E\xi}(r)]^* dr. \end{aligned} \tag{A2}$$

Superscript T denotes here the matrix transposition. Vectors $\mathbf{R}^{E\xi}(r)$ and $\mathbf{R}^{E'\xi'}(r)$ represent single eigensolutions of the coupled channel problem (18). Hence, it holds

$$\int_0^L [\mathbf{R}^{E'\xi'}(r)]^T\left\{-\frac{\hbar^2}{2m_e}\frac{d^2}{dr^2}\otimes\mathbf{I}+\mathbf{L}(r)+\mathbf{V}(r)-E\mathbf{I}\right\} \times[\mathbf{R}^{E\xi}(r)]^* dr=0; \tag{A3}$$

and

$$\int_0^L [\mathbf{R}^{E\xi}(r)]^{*T}\left\{-\frac{\hbar^2}{2m_e}\frac{d^2}{dr^2}\otimes\mathbf{I}+\mathbf{L}(r)+\mathbf{V}(r)-E'\mathbf{I}\right\} \times\mathbf{R}^{E'\xi'}(r)dr=0. \tag{A4}$$

Taking into account the symmetry of $\mathbf{V}(r)$ and $\mathbf{L}(r)$, and assuming that $E\neq E'$, one arrives to the formula

$$\begin{aligned} I_L(E,\xi,E',\xi') = \frac{\hbar^2}{2m_e}\frac{1}{(E-E')}\int_0^L\Big\{ & [\mathbf{R}^{E\xi}(r)]^{*T} \\ & \times\frac{d^2}{dr^2}\mathbf{R}^{E'\xi'}(r)-[\mathbf{R}^{E'\xi'}(r)]^T \\ & \times\frac{d^2}{dr^2}[\mathbf{R}^{E\xi}(r)]^*\Big\}dr. \end{aligned} \tag{A5}$$

Integration by parts and substitution of the inner boundary condition $\mathbf{R}^{E\xi}(0)=\mathbf{R}^{E'\xi'}(0)=\mathbf{0}$ enables us to express I_L in terms of local properties of the corresponding eigensolutions. One has

$$\begin{aligned} I_L(E,\xi,E',\xi') = \frac{\hbar^2}{2m_e}\frac{1}{(E-E')}\Big\{ & [\mathbf{R}^{E\xi}(L)]^{*T}\frac{d}{dr}\mathbf{R}^{E'\xi'}(L) \\ & -[\mathbf{R}^{E'\xi'}(L)]^T\frac{d}{dr}[\mathbf{R}^{E\xi}(L)]^*\Big\}. \end{aligned} \tag{A6}$$

From now on, the case of very large L is considered. The form of Eq. (16) implies that the radial components $R_q^{E\xi}(r)$ behave asymptotically as

$$R_q^{E\xi}(r\to\infty)=s_q^{E\xi}\sin(kr)+c_q^{E\xi}\cos(kr),\quad \text{with}\ \ k=(1/\hbar)\sqrt{2m_eE}. \tag{A7}$$

Coefficients $s_q^{E\xi}$ and $c_q^{E\xi}$ are unambiguously fixed with given choice of the outer boundary conditions. In particular, assuming the convention (21) and employing the asymptotic formulas $\mathsf{j}_l(x\to\infty)=+\sin(x-l\pi/2)/x$ and $\mathsf{n}_l(x\to\infty)=-\cos(x-l\pi/2)/x$, it follows that

$$s_q^{E\xi}=\sqrt{\frac{2m_e}{\pi\hbar^2k}}\{+\cos(l_q\pi/2)\,\delta_{q\xi}-\sin(l_q\pi/2)K_q^{E\xi}\}, \tag{A8}$$

$$c_q^{E\xi}=\sqrt{\frac{2m_e}{\pi\hbar^2k}}\{+\sin(l_q\pi/2)\,\delta_{q\xi}-\cos(l_q\pi/2)K_q^{E\xi}\}. \tag{A9}$$

Similarly, considering the convention (22) and exploiting the formula $\mathsf{h}_l^{\pm}(x\to\infty)=\mp i\exp[\pm i(x-l\pi/2)]/x$, one obtains

$$s_q^{E\xi}=(i^{l_q})\sqrt{\frac{m_e}{2\pi\hbar^2k}}\{\delta_{q\xi}+(-1)^{l_q+1}S_q^{E\xi}\}, \tag{A10}$$

$$c_q^{E\xi}=(i^{l_q+1})\sqrt{\frac{m_e}{2\pi\hbar^2k}}\{\delta_{q\xi}+(-1)^{l_q}S_q^{E\xi}\}. \tag{A11}$$

Combination of Eqs. (A6) and (A7) yields after straightforward manipulations the result

$$I_L(E,\xi,E',\xi')=\mathcal{S}^{(-)}\frac{\sin[(k-k')L]}{(k-k')}+\mathcal{S}^{(+)}\frac{\sin[(k+k')L]}{(k+k')}+\mathcal{C}^{(-)}\frac{\cos[(k-k')L]}{(k-k')}+\mathcal{C}^{(+)}\frac{\cos[(k+k')L]}{(k+k')}. \tag{A12}$$

Coefficients $\mathcal{S}^{(\pm)}$ and $\mathcal{C}^{(\pm)}$ are given by the expressions

$$\mathcal{S}^{(-)}=\frac{1}{2}\sum_q\,(+s_q^{E\xi*}s_q^{E'\xi'}+c_q^{E\xi*}c_q^{E'\xi'}), \tag{A13}$$

$$\mathcal{S}^{(+)}=\frac{1}{2}\sum_q\,(-s_q^{E\xi*}s_q^{E'\xi'}+c_q^{E\xi*}c_q^{E'\xi'}), \tag{A14}$$

$$\mathcal{C}^{(-)}=\frac{1}{2}\sum_q\,(-s_q^{E\xi*}c_{q'}^{E'\xi'}+c_q^{E\xi*}s_q^{E'\xi'}), \tag{A15}$$

$$\mathcal{C}^{(+)}=\frac{1}{2}\sum_q\,(-s_q^{E\xi*}c_q^{E'\xi'}-c_q^{E\xi*}s_q^{E'\xi'}). \tag{A16}$$

The overlap integral $I_L(E,\xi,E',\xi')$ is a well-defined continuous function of E and E', including cases of $E=E'$. The same is true for all the coefficients $\mathcal{S}^{(\pm)}$, $\mathcal{C}^{(\pm)}$ and consequently also for the first, the second and the fourth term from the right hand side of Eq. (A12). However, the function $\cos[(k-k')L]/(k-k')$ from the third term of Eq. (A23) exhibits a singularity at $E=E'$. Hence, the $\mathcal{C}^{(-)}$ coefficient must necessarily vanish for $E=E'$,

$$\sum_q\,(s_q^{E\xi*}c_q^{E\xi'}-c_q^{E\xi*}s_q^{E\xi'})=0. \tag{A17}$$

Condition (A17) holds for any pair of particular solutions of Eq. (18) with the same eigenvalue $E>0$. It is fulfilled trivially if $\xi=\xi'$. In the case of boundary conditions (21) or (22), general validity of relations (A17) for any pair of ξ, ξ' is easily verified by direct substitution of the expressions (A8), (A9), or (A10), (A11). We recall at this point that the **K** matrix is real and symmetric, $K_q^{E\xi}=K_\xi^{Eq}$, and that the **S** matrix is unitary, $\Sigma_q S_q^{E\xi*}S_q^{E\xi'}=\delta_{\xi\xi'}$.

The limit of $I_L(E,\xi,E',\xi')$ for $L\to\infty$ is to be investigated now. For large values of L, all the terms of Eq. (A12) behave as rapidly oscillating functions of E and E'. If $E\neq E'$, none of these four terms can provide any significant contribution to I_L as $L\to\infty$. In the case of $E=E'$, the only appreciable effect arises from the first term which diverges to infinity with increasing L. Introducing the Dirac delta function by a well-known formula

$$\delta(\xi)=\lim_{L\to\infty}\frac{\sin(\xi L)}{\pi\xi}, \tag{A18}$$

one obtains the result

$$I(E,\xi,E',\xi')=\lim_{L\to\infty}I_L(E,\xi,E',\xi')=\frac{\pi}{2}\left\{\sum_q\,s_q^{E\xi*}s_q^{E\xi'}+c_q^{E\xi*}c_q^{E\xi'}\right\}\delta(k-k'). \tag{A19}$$

Symbol $\delta(k-k')$ can be replaced by the delta function of energy via the relation

$$\delta(k-k')=\hbar\sqrt{(2E/m_e)}\,\delta(E-E'). \tag{A20}$$

Then,

$$I(E,\xi,E',\xi')=\frac{\pi\hbar}{\sqrt{2m_e}}\sqrt{E}\left\{\sum_q\,s_q^{E\xi*}s_q^{E\xi'}+c_q^{E\xi*}c_q^{E\xi'}\right\}\delta(E-E'). \tag{A21}$$

The quantity $I(E,\xi,E',\xi')$ can be identified with the scalar product $\langle\psi_{E\xi}(\mathbf{r})|\psi_{E'\xi'}(\mathbf{r})\rangle$. The generalized orthonormality relations (14), rewritten equivalently as

$$I(E,\xi,E',\xi')=\delta_{\xi\xi'}\delta(E-E'), \tag{A22}$$

are fulfilled if, and only if,

$$\frac{\pi\hbar}{\sqrt{2m_e}}\sqrt{E}\left\{\sum_q\,s_q^{E\xi*}s_q^{E\xi'}+c_q^{E\xi*}c_q^{E\xi'}\right\}=\delta_{\xi\xi'}. \tag{A23}$$

For the asymptotic convention (A22) it is straightforward to show that the condition (A23) is indeed satisfied. One has to substitute the expressions (A10), (A11) and to employ unitarity of the **S** matrix. Different conclusion is found when the

functional form (A21) is considered. After insertion of the formulas (A8) and (A9), the left hand side of Eq. (A23) equals to $(\delta_{\xi\xi'}+\Sigma_q K_q^{E\xi}K_q^{E\xi'})$ and is in general nonzero even for $\xi\neq\xi'$. In order to fulfill the relations (A23), it is unavoidable in this case to perform an additional linear transformation

$$\phi_{E\eta}(\mathbf{r})=\sum_{\xi}\lambda_{\eta\xi}\psi_{E\xi}(\mathbf{r}). \tag{A24}$$

In practice, such linear combinations can be easily constructed, e.g., using the Gramm–Schmidt orthonormalization procedure.[26]

[1] C. Desfrancois, H. Abdoul-Carime, and J.-P. Schermann, Int. J. Mod. Phys. B **10**, 1339 (1996).
[2] M. Gutowski and P. Skurski, Recent Res. Devel. Physical Chem. **3**, 245 (1999).
[3] K. D. Jordan and J. J. Wendoloski, Chem. Phys. **21**, 145 (1977).
[4] D. M. Chipman, J. Phys. Chem. **83**, 1657 (1979).
[5] M. Armbruster, H. Haberland, and H.-G. Schindler, Phys. Rev. Lett. **47**, 323 (1981).
[6] J. V. Coe, G. H. Lee, J. G. Eaton, S. T. Arnold, H. W. Sarkas, K. H. Bowen, C. Ludewigt, H. Haberland, and D. R. Worsnop, J. Chem. Phys. **92**, 3980 (1990).
[7] J. H. Hendricks, H. L. de Clerq, S. A. Lyapustina, and K. H. Bowen, J. Chem. Phys. **107**, 2962 (1997).
[8] W. R. Garrett, J. Chem. Phys. **77**, 3666 (1982).
[9] D. C. Clary, J. Phys. Chem. **92**, 3173 (1988).
[10] R. N. Barnett, U. Landman, C. L. Cleveland, and J. Jortner, J. Chem. Phys. **88**, 4421 (1988).
[11] H. Abdoul-Carime and C. Desfrancois, Eur. Phys. J. D **2**, 149 (1998).
[12] D. Clary and D. M. Benoit, J. Chem. Phys. **111**, 10559 (1999).
[13] P. Jungwirth and V. Spirko, Phys. Rev. Lett. **84**, 1140 (2000).
[14] M. Gutowski, K. D. Jordan, and P. Skurski, J. Phys. Chem. A **102**, 2624 (1998).
[15] M. Gutowski and P. Skurski, J. Chem. Phys. **107**, 2968 (1997).
[16] M. Gutowski and P. Skurski, J. Phys. Chem. B **101**, 9143 (1997).
[17] S. B. Suh, H. M. Lee, J. Kim, J. Y. Lee, and K. S. Kim, J. Chem. Phys. **113**, 5273 (2000).
[18] J. Kim, S. B. Suh, and K. S. Kim, J. Chem. Phys. **111**, 10077 (1999).
[19] J. Kim, J. Y. Lee, K. S. Oh, J. M. Park, S. Lee, and K. S. Kim, Phys. Rev. A **59**, R930 (1999).
[20] H.-Y. Chen and W.-S. Sheu, J. Chem. Phys. **110**, 9032 (1999).
[21] R. Rameakers, D. M. A. Smith, Y. Elkadi, and L. Adamowicz, Chem. Phys. Lett. **277**, 269 (1997).
[22] F. Wang and K. D. Jordan, J. Chem. Phys. **114**, 10717 (2001).
[23] F. Wang and K. D. Jordan, J. Chem. Phys. **116**, 6973 (2002).
[24] M. Hliwa, J. C. Barthelat, and J. P. Malrieu, J. Phys. B **18**, 2433 (1985).
[25] M. Hliwa and J.-P. Daudey, Chem. Phys. Lett. **153**, 471 (1988).
[26] A. Messiah, *Quantum Mechanics*, Vol. 1 (New Holland, Amsterdam, 1961).
[27] B. R. Johnson, J. Chem. Phys. **69**, 4678 (1978).
[28] A. Ralston, *A First Course in Numerical Analysis* (McGraw-Hill, New York, 1965).
[29] E. Fermi and E. Teller, Phys. Rev. **72**, 406 (1947).
[30] J. E. Turner, Am. J. Phys. **45**, 758 (1977).
[31] M. R. H. Rudge, J. Molec. Phys. **11**, 1497 (1978).
[32] M. S. Child, *Molecular Collision Theory* (Academic, London, 1974), Appendix A, pp. 236–237.